Single-Molecule AFM Characterization of Individual Chemically Tagged DNA Tetrahedra

ARTICLE *in* ACS NANO · AUGUST 2011

Impact Factor: 12.88 · DOI: 10.1021/nn201705p · Source: PubMed

Single-Molecule AFM Characterization of Individual Chemically Tagged DNA Tetrahedra

Michael Leitner,[†] Nick Mitchell,[‡] Markus Kastner,[†] Robert Schlapak,[§] Hermann J. Gruber,[†] Peter Hinterdorfer,[†,§] Stefan Howorka,[‡,§] and Andreas Ebner[†,*]

[†]Institute for Biophysics, Johannes Kepler University, A-4040 Linz, Austria, [‡]Department of Chemistry, Institute of Structural Molecular Biology, University College London, London WC1H 0AJ, U.K., and [§]Center for Advanced Bioanalysis, Upper Austrian Research GmbH, A-4020 Linz, Austria

ABSTRACT Single-molecule characterization is essential for ascertaining the structural and functional properties of bottom-up DNA nanostructures. Here we enlist three atomic force microscopy (AFM) techniques to examine tetrahedron-shaped DNA nanostructures that are functionally enhanced with small chemical tags. In line with their application for biomolecule immobilization in biosensing and biophysics, the tetrahedra feature three disulfide-modified vertices to achieve directed attachment to gold surfaces. The remaining corner carries a single bioligand that can capture and present individual cargo biomolecules at defined lateral nanoscale spacing. High-resolution AFM topographic imaging confirmed the directional surface attachment as well as the highly effective binding of individual receptor molecules to the exposed bioligands. Insight into the binding behavior at the single-molecule level was gained using molecular recognition force spectroscopy using an AFM cantilever tip with a tethered molecular receptor. Finally, simultaneous topographic and recognition imaging demonstrated the specific receptor–ligand interactions on individual tetrahedra. In summary, AFM characterization verified that the rationally designed DNA nanostructures feature characteristics to serve as valuable immobilization agents in biosensing, biophysics, and cell biology.

KEYWORDS: DNA nanotechnology · atomic force microscopy · force spectroscopy · recognition imaging · chemical biology

The formation of defined DNA-based nanomolecular structures from the bottom up is an exciting area of research that can contribute to materials science, biomedical diagnostics, and cell biology.[1] One increasingly popular trend within DNA nanotechnology is to use chemical tags to functionally enhance the nanostructures. For instance, multiple dye molecules have been arranged into arrays to improve the efficiency of light absorption and to allow fine-tuning of the emission wavelength.[2] In addition, aromatic metal-binding sites have been engineered into a DNA lattice to help arrange metallic nanoparticles into a 3D array that exhibits new collective properties.[3] An important aspect is the single-molecule characterization of native and chemically enhanced DNA nanostructures to confirm their structural and functional properties.[4–9] One widely used tool for structural examination is electron microscopy in combination with negative staining. Atomic force microscopy (AFM) is also a popular and powerful approach, as it helps to confirm the predicted dimensions, shape, and nanomechanical properties of DNA nanostructures at the single-molecule level at or near physiological conditions.[5,6,9] Despite the availability of analysis tools, the examination of chemically tagged DNA nanoarchitectures remains challenging, as the small organic moieties cannot be directly visualized. One route to overcome this hurdle is to employ recognition-based AFM techniques in which a cantilever tip carries a molecular receptor that recognizes the chemical tags.[10,11] This strategy has been successfully applied in DNA sensing to detect small methyl groups in linear sequences that are of relevance in biodiagnostics.[12] However, chemically altered DNA nanostructures have so far not been examined with recognition-based imaging. Here we demonstrate that individual chemically modified DNA nanostructures can be functionally characterized with topographic and recognition-based AFM.

As model system for our single-molecule investigation, we selected chemically enhanced DNA tetrahedra whose defined functional properties are of interest in applications involving the surface immobilization of biomolecules. DNA tetrahedra are nanostructures that are composed of double-stranded DNA (Figure 1A). The self-assembly objects are formed by annealing four single-stranded DNA oligonucleotides (ssDNA) each carrying three different complementary sequence blocks (Figure 1A).[5,13] The dimensions of the DNA tetrahedron depend on the size of the ssDNA. For example, four 55-nt strands yield 5.8 nm long tetrahedron

* Address correspondence to andreas.ebner@jku.at.

Received for review May 10, 2011 and accepted July 28, 2011.

Published online July 28, 2011
10.1021/nn201705p

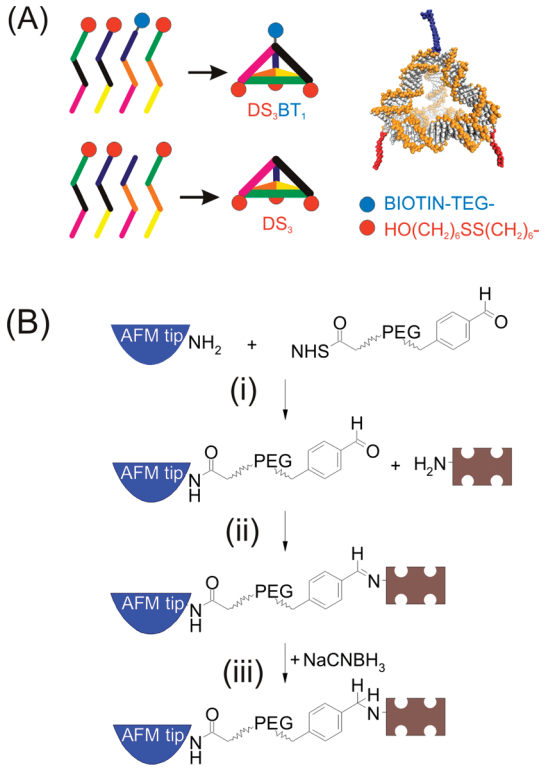

Figure 1. DNA tetrahedra design and tip chemistry. (A) The molecular self-assembly of four 5′-functionalized DNA oligonucleotides yields DNA tetrahedra DS_3BT_1 and DS_3 carrying disulfide groups at three vertices. The optional biotin tag is linked *via* a flexible tri(ethylene glycol) (TEG) spacer to the forth vertex of DS_3BT_1. (B) Stepwise functionalization of the amino-derivatized AFM tip using the cross-linker aldehyde-PEG-NHS, streptavidin, and $NaCNBH_3$.

edges. In the assembled form, the free 5′ termini of the ssDNA are positioned at the vertices of the tetrahedron (Figure 1A). By using 5′ chemically modified ssDNA, the tetrahedron corners can be equipped with groups that impart the nanostructure with defined functional properties. Using this strategy, we have previously created a rationally designed tetrahedron termed DS_3BT_1, which carries three disulfide (DS) legs and one biotin tag at the vertices (Figure 1A)[14] and therefore has the potential to bind onto gold surfaces in an orientated fashion while presenting individual bioaffinity tags at defined nanoscale spacing, which is optimal for molecular recognition. In general, exposing surface-tethered biomolecular ligands to the ambient is relevant and may be exploited when DNA tetrahedra are used as immobilization agents for applications in biosensing, cell biology, or biophysics. For example, other biomolecular receptors such as DNA strands could be displayed at the tip of the tetrahedron, thereby reducing undesired steric crowding between receptors, as well as close contact to the solid substrate, which can negatively influence recognition. In the present study, we demonstrate that DNA tetrahedra display the anticipated favorable characteristics. Three AFM techniques are used to examine the structure of DNA tetrahedron DS_3BT_1 and test whether the biotin affinity tag at the tip of the gold-immobilized structure is sterically accessible. The outcome of the study paves the way for further work in which chemically engineered tetrahedra are exploited as an immobilization agent.

RESULTS AND DISCUSSION

DNA tetrahedron DS_3BT_1 was formed *via* self-assembly by heating and cooling a mixture of four 55 nt long DNA oligonucleotides as described in the Methods section. We also generated DNA tetrahedron DS_3, which lacks the biotin moiety (Figure 1A). The successful formation of the self-assembled structures was confirmed using gel electrophoresis.[15]

We applied three different AFM techniques to examine whether DNA tetrahedron DS_3BT_1 is able to specifically and efficiently bind streptavidin molecules; molecular recognition force spectroscopy (MRFS) was used first, as this technique is a powerful tool to characterize biomolecular recognition at the single-molecule level.[16−21] In MRFS, individual molecular recognition events are detected between a receptor-coated AFM tip and surface-tethered ligand (or *vice versa*), resulting in molecular unbinding forces. Second, DNA tetrahedra were characterized using topographic imaging under near-physiological conditions. In particular, binding of individual streptavidin proteins onto the top of the tetrahedra was detected by measuring the height differences relative to the naked nanostructures. Third, *via* simultaneous topographic and recognition (TREC) imaging[10,11,22] we probed the interaction of surface-bound molecules and complementary binding partners tethered to the AFM tip.

Molecular Recognition Force Spectroscopy. For the characterization of biotinylated DS_3BT_1, AFM tips were derivatized with single streptavidin molecules (Figure 1B). The functionalization of sharp silicon nitride AFM tips followed an established protocol. After amino functionalization with ethanolamine,[18,20] streptavidin was bound in a three-step procedure.[18] In the first step (Figure 1B, i), linker NHS-PEG-aldehyde was coupled to the amine groups, forming an amide bond. The aldehyde function was subsequently used to attach streptavidin *via* the primary amine groups of the lysine residues, resulting in a Schiff base (Figure 1B, ii). After inactivating the remaining aldehyde groups using a short amine linker (not shown), the Schiff base was stabilized by reduction using $NaCNBH_3$ as hydride donor (Figure 1B, iii).

The streptavidin-functionalized tips were applied in MRFS experiments to capture the biotin moiety of DS_3BT_1 tetrahedra (Figure 2A). After immobilizing DNA tetrahedra on atomically flat template-stripped gold (TSG),[23−25] individual molecular recognition events between tip-tethered proteins and the DNA structures

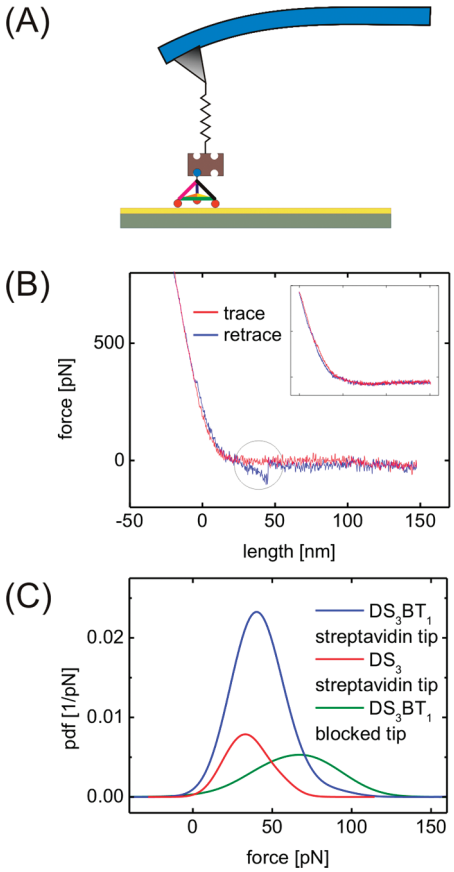

Figure 2. Single-molecule interaction force measurements. (A) A streptavidin-modified AFM tip interacts with the DS_3BT_1-coated sample surface in the MRFS experiment. (B) A typical force distance cycle for experiment. An unbinding event with an unbinding length of ~27 nm and a rupturing force of ~50 pN is highlighted by a circle. No unbinding event occurs after blocking the interaction with free biotin molecules (inset). (C) Probability density function (pdf) generated from 1000 force distance cycles for the interaction with DS_3BT_1 (blue line) and, for control purposes, of a biotin-blocked streptavidin tip (green line) and of tetrahedra DS_3 without biotin residue (red line). The areas of the pdfs of the specificity proof experiments were normalized with respect to their binding probability.

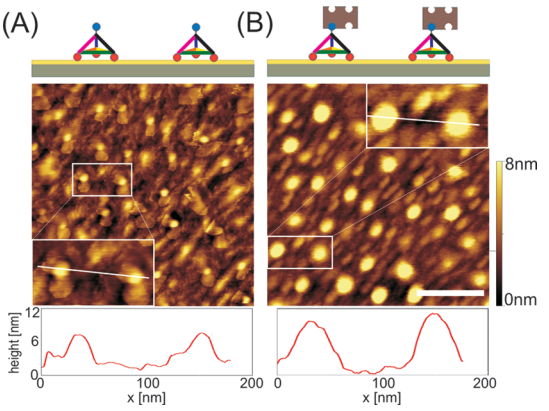

Figure 3. Topographic AFM imaging of individual tetrahedra and tetrahedron–streptavidin complexes. (A) Topographical AFM image of DS_3BT_1 on template-stripped gold with a surface density of ~60 tetrahedra/μm^2. (B) Tetrahedra after binding of a streptavidin molecule. The insets show the same two tetrahedra as in (A) and (B) representing the height increase after binding of a streptavidin. Due to the drift during the incubation time, the whole areas of (A) and (B) are not the same. Individual DNA tetrahedra had a height of at least 4.1 nm and a diameter of about 14.5 nm. DS_3BT_1 that bound single streptavidin molecules were increased in height by 3 nm. Analysis showed that 91% of the tetrahedra captured a streptavidin molecule. The 200 nm scale bar and the *z* scaling are for both images.

were recorded in force distance cycles (FDCs), as shown in Figure 2B. In a FDC, the tip is brought into contact with the gold surface, leading to the upward bending of the cantilever, as indicated by the constant increase of resisting force in the FDC trace (Figure 2B, red line). Upon retraction, the distance between the AFM tip and gold surface increases until the molecular bond between the streptavidin-coated tip and a biotinylated DS_3BT_1 tetrahedron ruptures, leading to a characteristic cantilever deflection (Figure 2B, blue line, circle). Blocking the molecular recognition by addition of biotin abolished the characteristic unbinding deflection (Figure 2B, inset).

More than 1000 traces were statistically evaluated to yield probability density functions (Figure 2C). The function for the interaction between streptavidin and DS_3BT_1 (Figure 2C, blue line) shows a clear maximum of 40 pN as the most probable unbinding force with a binding probability of 19%. A value of 40 pN is in line with literature studies on biotin–strepavidin rupture forces. By comparison, control experiments using either biotin-blocked streptavidin or biotin-free DS_3 tetrahedra displayed lower interaction probabilities of 7% and 6% (Figure 2C, red and green line, respectively), thereby verifying that the interaction between streptavidin and biotinylated DS_3BT_1 was specific. The values for the binding probabilities of the control experiments are typical for this technique[18,19,26] and can be explained by unspecific adhesion and/or incomplete block. Nonspecific adhesion forces can thereby be slightly lower or higher compared to specific recognition.

Topographical AFM Imaging. The capturing efficiency of biotin-functionalized tetrahedra for individual streptavidin molecules was determined by AFM imaging. DS_3BT_1 tetrahedra were immobilized on TSG surfaces *via* their disulfide legs (Figure 3A, top) at a surface density of DS_3BT_1 that was lower than in the previous unbinding experiments in order to facilitate the unambiguous identification of individual tetrahedra *via* AFM dynamic force mode imaging. For the identification of separate tetrahedra, thresholds for the height and diameter were applied. The thresholds were based on the tetrahedra dimensions[14] taking into account height compression by an AFM tip[15] as well as tip broadening (see Methods section). The acceptable dimensions were 3–4.5 nm for the height and 11–17 nm for the diameter. Applying these boundaries helped detect DNA tetrahedra (Figure 3A, inset, cross section) with an average height of 4.16 ± 0.46 nm and diameter of

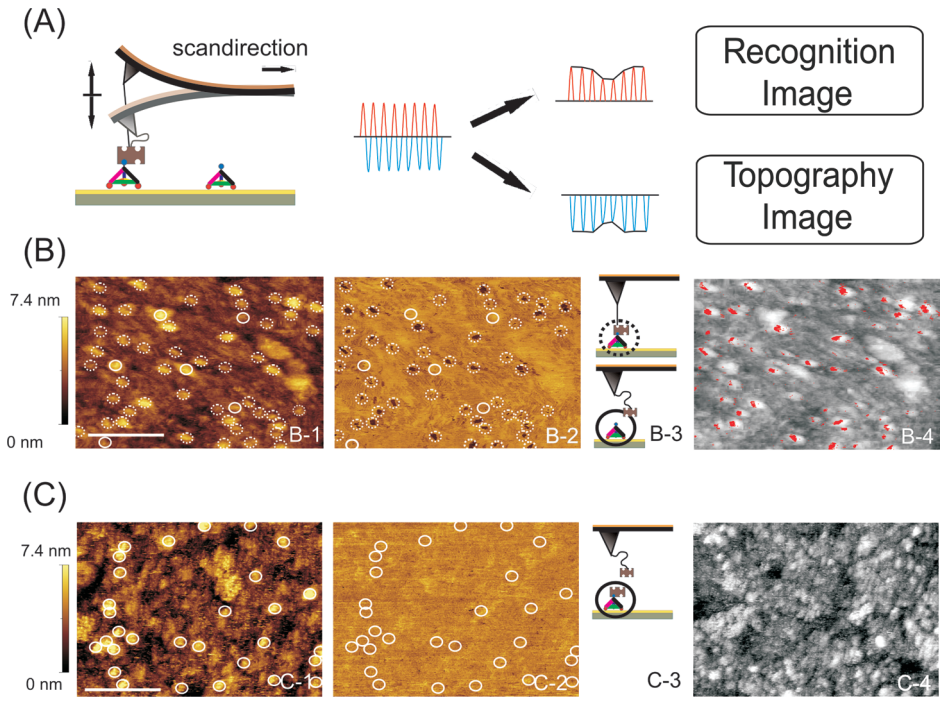

Figure 4. Simultaneous topographic and recognition imaging of DS_3BT_1 tetrahedra on gold surfaces. (A) Schematic drawing of the TREC imaging principle. Dotted circles mark tetrahedra with recognition (B1, B2). The solid circles represent tetrahedra without recognition (B-1, B-2) and for streptavidin-blocked tetrahedra (C-1, C-2). An overlay of topographic image with red recognition signals (B-4) demonstrates that addition of streptavidin blocks biotinylated tetrahedra (C-4). The scale bar is 200 nm.

14.5 ± 2.9 nm. To quantify the binding of streptavidin to the biotin tips, protein was added to the gold surfaces to form DS_3BT_1–streptavidin complexes (Figure 3B, top). As the same surface area was imaged before and after addition of streptavidin, the enlarged topographical signals (Figure 3B, inset, cross section) could be assigned to individual tetrahedron–streptavidin complexes. The height for a complex was increased by 3.14 ± 1.24 nm compared to single tetrahedra, in line with the molecular dimension of streptavidin[27] and previous height measurements of the protein with AFM.[14] Analysis of the images showed that 91% of all tetrahedra bound streptavidin, which means a binding ratio of streptavidin per biotin (SA/B) of 0.91. This is larger than the binding ratio of 0.38 of conventional flat biotinylated surfaces such as self-assembled monolayers[28] as well as of substrates with optimized biotin spacing (0.76)[29] and with rationally designed tripods (0.32) that are meant to improve recognition[28] (see Table S2 in the Supporting Information).

Topography and Recognition Imaging. The simultaneous topographic and recognition detection of individual biotin tags on DS_3BT_1 tetrahedra was examined with streptavidin-modified AFM tips and TREC imaging. In TREC, an oscillating cantilever scans over the sample surface, giving rise to an oscillating amplitude read-out (Figure 4A).[10,11,22] Similar to conventional topographic imaging, individual molecules on a solid substrate surface block the downward movement of the AFM tip, thereby shifting up the troughs in the amplitude oscillations. By contrast, molecular recognition between the surface-bound biotin tags and the AFM-tethered streptavidin receptors limits the upward movement of the cantilever, leading to lowered peaks in the amplitude oscillations (Figure 4A).

TREC imaging of DS_3BT_1 on a gold surface yielded simultaneously acquired topography (Figure 4B-1) and recognition images (Figure 4B-2). Single tetrahedra and tetrahedra–streptavidin complexes in the topographic images were identified by applying the previously defined thresholds. Similarly, the automated detection of the recognition spots was based on a threshold value that is 5 times higher than the average noise within the recognition image. The results of this analysis are visually encoded in Figure 4B. Dotted circles highlight individual tetrahedra with elevated topographic height (Figure 4B-1 and B-3), while dark spots reflect successful molecular recognition between cantilever-tethered streptavidin and the biotin residue of DS_3BT_1 (Figure 4B-2 and B-3). To facilitate comparison between the topographic and recognition signals, a composite image was generated by overlaying the recognition mask onto the topography image (Figure 4B-4, recognition signals in red). The overlay confirmed that most DNA tetrahedra were successfully recognized in TREC. Indeed, Spareman's rank correlation coefficient ρ was found to be 0.151, which strongly indicates a correlation between topographic and recognition signals.[30] The specificity of the recognition was demonstrated by blocking the biotin moieties with

streptavidin, which was added to DS_3BT_1 surfaces. In line with a specific block, DNA tetrahedra that were detected in the topographic image (Figure 4C-1) did not give rise to specific signals in the recognition image (Figure 4C-2). Numeric analysis of a total of six TREC images proved that 88.5% of 378 tetrahedra gave a recognition signal before the block, while after protein addition only 4.4% among 453 tetrahedra gave a signal.

CONCLUSIONS

This report demonstrates that DNA tetrahedra represent new heterobifunctional adapters for positioning of individual protein molecules at defined lateral spacing on flat surfaces. The ability to address laterally resolved individual molecules is of considerable interest in single-molecule biophysics. Furthermore, immobilizing biomolecules on surfaces at defined lateral distance and in an oriented fashion is also of relevance in biosensing and molecular recognition at surfaces. Usually, the conventional immobilization of molecular receptors at undefined spacing and in random orientation can result in poor recognition and specificity due to undesired steric crowding and limited access when the receptors are too close to the substrate surface.[31] The use of DNA tetrahedra as linkers may address these issues, as the biomolecular receptor is present at the top of the oriented bound tetrahedron. Indeed, most likely due to the high steric accessibility of the biotin tag at the tip of DS_3BT_1, we report here a higher surface ratio of bound streptavidin per biotin than biotinylated SAMs or biotinylated dendrons.[28,32,33] On the basis of the findings we expect that the DNA nanostructures can act in general as immobilization agents that improve biomolecular recognition and overcome problems in conventional surface-immobilization approaches. Experiments to provide evidence of the comparative advantage of the tetrahedron strategy over conventional immobilization routes are underway. In addition, our report demonstrates that recognition-based AFM techniques such as MRFS and TREC are excellent tools for detecting and exactly localizing individual chemical tags within man-made DNA nanostructures. In conclusion, our report advances the field of DNA nanotechnology by chemically enhancing DNA tetrahedra with chemical tags and providing valuable tools for characterization of nanostructures at the single-molecule level.

METHODS

DNA Tetrahedra. The design and formation of the DNA tetrahedra was performed in close analogy to Goodman *et al.*[5,13] following a procedure by Mitchell *et al.*[15] Briefly, four different oligonucleotides 55 nt in length were annealed to obtain the DNA tetrahedra. The DNA strands carried disulfides (DS) or biotin (BT) tags at the 5′ terminus. Tetrahedron DS_3BT_1 was formed by annealing three disulfide-labeled and one biotinylated oligonucleotide, whereas DS_3 was generated using three disulfide-labeled and one unlabeled oligonucleotide. The integrity and purity of DS_3BT_1 and DS_3 were proven by gel electrophoresis as described by Mitchell *et al.*[15] A more detailed description of the formation and gel analysis of the tetrahedra is given in the Supporting Information.

Surface Preparations. Template-stripped gold surfaces were prepared as described by Hegner *et al.*[34] The silicon template chips were glued using an EpoTek 377 epoxide glue (Polytec PT GmbH, Waldbronn, Germany) to the gold-coated mica. The mica−gold interface was cleaved using tetrahydrofuran and used immediately afterward. Statistically dense layers of thiolated tetrahedra to be used for molecular recognition force spectroscopy measurements were generated by incubating TSG chips with 240 nM DS_3BT_1 in buffer A (1 mM Tris, 1 mM NaCl, 10 μM EDTA, pH 8.0) for 30 min. Preparations with lower surface coverage were achieved using 2.4 nM DS_3BT_1 in buffer B (0.01 mM Tris, 0.01 mM NaCl, 0.1 μM EDTA, pH 8.0). After incubation, TSG chips were cleaned extensively by rinsing with ultrapure water and used immediately afterward.

AFM Tip Functionalization. For molecular recognition force spectroscopy, chemically inert oxide-sharpened silicon nitride AFM tips (MSCT-AUHW, Veeco, USA) were used. For simultaneous topography and recognition imaging magnetically coated silicon nitride cantilevers with silicon tips (Agilent Technologies, type VI MACLevers, USA) were employed. Both were functionalized as described. Tips of both types were cleaned with ethanol (3 × 5 min) and chloroform (3 × 5 min) and dried in a gentle nitrogen stream. The tips were then incubated with 0.55 g/mL ethanolamine hydrochloride in DMSO in the presence of molecular sieves (3 Å) at room temperature to generate reactive amino groups on the tip surface. Subsequently, the heterobifunctional cross-linker NHS-PEG-aldehyde was covalently coupled to the amino-derivatized surface by immersing cantilevers into a solution of 3.3 mg of NHS-PEG-aldehyde cross-linker dissolved in 0.5 mL of chloroform. As catalyst, 10 μL of triethylamine was added to start the reaction. After 2 h reaction, the tips were washed with chloroform (3 × 5 min) and dried in a gentle stream of nitrogen. The functionalization of cantilevers with streptavidin was achieved by immersing the AFM tips in 100 μL of PBS buffer (150 mM NaCl, 5 mM NaH_2PO_4) supplemented with 0.2 mg/mL streptavidin and 2 μL of $NaCNBH_3$ solution (32 mg of $NaCNBH_3$ dissolved in 500 μL of 10 mM NaOH). Ten minutes prior to washing the tips, 5 μL of 1 M ethanolamine hydrochloride was added to the solution in order to inactivate remaining aldehyde groups. The tips were washed with PBS buffer (3 × 5 min) and stored in the same buffer at 4 °C for up to three days.

Molecular Recognition Force Spectroscopy. All AFM measurements were performed on a Pico SPM Plus setup including MAC and TREC Box (Molecular Imaging, Tempe, AZ, USA) under aqueous conditions. For MRFS, a streptavidin-functionalized AFM tip was repeatedly exposed to a surface densely covered with tetrahedra (~25 000 tetrahedra/μm^2). Force distance cycles were acquired in PBS buffer. The scan rate was 1 s at a *z*-range of 200 nm. The used cantilevers had a nominal spring constant between 10 and 30 pN/nm. The actual spring constant was determined according to Hutter *et al.*[35] using the thermal noise method. For statistical data evaluation ~1000 FDCs were collected at the same piezo velocity. The data were weighted by their standard deviations to generate the probability density function. For each data point, the unbinding force and the corresponding standard deviation were used to construct a Gaussian distribution. The Gaussian distributions were then summed up, resulting in the final pdf. To proof the specificity of the molecular interaction, the streptavidin-functionalized AFM tip was blocked by external incubation in a solution of 0.2 mg/mL

biotin for 1 h. As additional control, force distance cycles were also conducted using a streptavidin-functionalized AFM tip and a dense layer of DNA tetrahedra without biotin vertex (DS_3).

AFM Imaging. For the topographic detection of individual DNA nanostructures, DS_3BT_1 tetrahedra were immobilized at a low surface coverage on gold slides ($\sim 100/\mu m^2$). The AFM measurements were conducted in tapping mode using a cantilever acceleration frequency of ~10 kHz. The scanning frequency was set to 1 Hz, and cantilevers had a nominal spring constant of 100 pN/nm. Experiments on the addressability of single DNA tetrahedra were conducted by injecting a streptavidin solution (50 μg/mL) during imaging. The position of the sample was held constant during the incubation step and imaging process.

Simultaneous Topography and Recognition Imaging. TREC imaging was conducted using a magnetically coated and streptavidin-functionalized AFM cantilever with a spring constant of 292 pn/nm. Gold surfaces with DNA tetrahedra ($\sim 100/\mu m^2$) were scanned at a frequency of 1 Hz in the MAC mode. The working amplitude was set to 15 nm. This resulted in a detectable amplitude reduction but is low enough to avoid unwanted rupturing of the complex.[36] Specificity proof experiments were performed by injecting a streptavidin solution (50 μg/mL) during imaging.

Acknowledgment. This work was supported by FFG MNT-era.net (project 823980) and by the Austrian Science Foundation (project N00104-NAN) and the state of Upper Austria. We thank Christian Rankl for help in data evaluation.

Supporting Information Available: Sequence of the DNA oligonucleotides, formation of the DNA tetrahedron, and biotin surface density analysis for optimized biotin/streptavidin ratio. This material is available free of charge *via* the Internet at http://pubs.acs.org.

REFERENCES AND NOTES

1. Lin, C.; Yan, H. DNA Nanotechnology: A Cascade of Activity. *Nat. Nanotechnol.* **2009**, *4*, 249–254.
2. Özhalici Unal, H.; Armitage, B. A. Fluorescent DNA Nanotags Based on a Self-Assembled DNA Tetrahedron. *ACS Nano* **2009**, *3*, 425–433.
3. Yang, H.; McLaughlin, C. K.; Aldaye, F. A.; Hamblin, G. D.; Rys, A. Z.; Rouiller, I.; Sleiman, H. F. Metal–Nucleic Acid Cages. *Nat. Chem.* **2009**, *1*, 390–396.
4. Ding, B.; Seeman, N. C. Operation of a DNA Robot Arm Inserted into a 2D DNA Crystalline Substrate. *Science* **2006**, *314*, 1583–1585.
5. Goodman, R. P.; Schaap, I. A.; Tardin, C. F.; Erben, C. M.; Berry, R. M.; Schmidt, C. F.; Turberfield, A. J. Rapid Chiral Assembly of Rigid DNA Building Blocks for Molecular Nanofabrication. *Science* **2005**, 1661–1665.
6. Mao, C.; Sun, W.; Shen, Z.; Seeman, N. C. A Nanomechanical Device Based on the B-Z Transition of DNA. *Nature* **1999**, *397*, 144–146.
7. Niemeyer, C. M.; Mirkin, C. A. *Nanobiotechnology: Concepts, Applications and Perspectives*; John Wiley & Sons: New York, 2004.
8. Rinker, S.; Ke, Y. G.; Liu, Y.; Chhabra, R.; Yan, H. Self-assembled DNA Nanostructures for Distance-dependent Multivalent Ligand-Protein Binding. *Nat. Nanotechnol.* **2008**, *3*, 418–422.
9. Rothemund, P. W. Folding DNA to Create Nanoscale Shapes and Patterns. *Nature* **2006**, *440*, 297–302.
10. Stroh, C. M.; Ebner, A.; Geretschlager, M.; Freudenthaler, G.; Kienberger, F.; Kamruzzahan, A. S. M.; Smith-Gill, S. J.; Gruber, H. J.; Hinterdorfer, P. Simultaneous Topography and Recognition Imaging Using Force Microscopy. *Biophys. J.* **2004**, *87*, 1981–1990.
11. Ebner, A.; Kienberger, F.; Kada, G.; Stroh, C. M.; Geretschlager, M.; Kamruzzahan, A. S. M.; Wildling, L.; Johnson, W. T.; Ashcroft, B.; Nelson, J.; *et al*. Localization of Single Avidin-biotin Interactions using Simultaneous Topography and Molecular Recognition Imaging. *ChemPhysChem* **2005**, *6*, 897–900.
12. Zhu, R.; Howorka, S.; Proll, J.; Kienberger, F.; Preiner, J.; Hesse, J.; Ebner, A.; Pastushenko, V. P.; Gruber, H. J.; Hinterdorfer, P. Nanomechanical Recognition Measurements of Individual DNA Molecules Reveal Epigenetic Methylation Patterns. *Nat. Nanotechnol.* **2010**, *5*, 788–791.
13. Goodman, R. P.; Berry, R. M.; Turberfield, A. J. The Single-Step Synthesis of a DNA Tetrahedron. *Chem. Commun.* **2004**, 1372–1373.
14. Mitchell, N.; Schlapak, R.; Kastner, M.; Armitage, D.; Chrzanowski, W.; Riener, J.; Hinterdorfer, P.; Ebner, A.; Howorka, S. A DNA Nanostructure for the Functional Assembly of Chemical Groups with Tunable Stoichiometry and Defined Nanoscale Geometry. *Angew. Chem., Int. Ed.* **2009**, 525–527.
15. Mitchell, N.; Schlapak, R.; Kastner, M.; Armitage, D.; Chrzanowski, W.; Riener, J.; Hinterdorfer, P.; Ebner, A.; Howorka, S. A DNA Nanostructure for the Functional Assembly of Chemical Groups at Tuneable Stoichiometry and Defined Nanoscale Geometry. *Angew. Chem., Int. Ed.* **2009**, *48*, 525–527.
16. Florin, E. L.; Moy, V. T.; Gaub, H. E. Adhesion Forces between Individual Ligand-Receptor Pairs. *Science* **1994**, *264*, 415–417.
17. Hinterdorfer, P.; Baumgartner, W.; Gruber, H. J.; Schilcher, K.; Schindler, H. Detection and Localization of Individual Antibody-Antigen Recognition Events by Atomic Force Microscopy. *Proc. Natl. Acad. Sci.* **1996**, *93*, 3477–3481.
18. Ebner, A.; Hinterdorfer, P.; Gruber, H. J. Comparison of Different Aminofunctionalization Strategies for Attachment of Single Antibodies to AFM Cantilevers. *Ultramicroscopy* **2007**, *107*, 922–927.
19. Ebner, A.; Kienberger, F.; Huber, C.; Kamruzzahan, A. S. M.; Pastushenko, V. P.; Tang, J.; Kada, G.; Gruber, H. J.; Sleytr, U. B.; Sára, M.; *et al*. Atomic Force Microscopy Imaging and Molecular Recognition Force Microscopy of Recrystallized Heterotetramers Comprising an S-layer-Streptavidin Fusion Protein. *ChemBioChem* **2006**, *7*, 588–591.
20. Riener, C. K.; Stroh, C. M.; Ebner, A.; Klampfl, C.; Gall, A. A.; Romanin, C.; Lyubchenko, Y. L.; Hinterdorfer, P.; Gruber, H. J. Simple Test System for Single Molecule Recognition Force Microscopy. *Anal. Chim. Acta* **2003**, *479*, 59–75.
21. Lee, G. U.; Kidwell, D. A.; Colton, R. J. Sensing Discrete Streptavidin-Biotin Interactions with Atomic Force Microscopy. *Langmuir* **1994**, *10*, 354–357.
22. Stroh, C.; Wang, H.; Bash, R.; Ashcroft, B.; Nelson, J.; Gruber, H.; Lohr, D.; Lindsay, S. M.; Hinterdorfer, P. Single-Molecule Recognition Imaging Microscopy. *Proc. Natl. Acad. Sci.* **2004**, *101*, 12503–12507.
23. Blackstock, J. J.; Li, Z. Y.; Freeman, M. R.; Stewart, D. R. Ultra-Flat Platinum Surfaces from Template-Stripping of Sputter Deposited Films. *Surf. Sci.* **2003**, *546*, 87–96.
24. Medalia, O.; Englander, J.; Guckenberger, R.; Sperling, J. AFM Imaging in Solution of Protein-DNA Complexes Formed on DNA Anchored to a Gold Surface. *Ultramicroscopy* **2002**, *90*, 103–112.
25. Hegner, M.; Wagner, P.; Semenza, G. Ultralarge Atomically Flat Template-Stripped Au Surfaces for Scanning Probe Microscopy. *Surf. Sci.* **1993**, *1993*, 39–46.
26. Ebner, A.; Wildling, L.; Kamruzzahan, A. S. M.; Rankl, C.; Wruss, J.; Hahn, C. D.; Holzl, M.; Zhu, R.; Kienberger, F.; Blaas, D.; *et al*. A New, Simple Method for Linking of Antibodies to Atomic Force Microscopy Tips. *Bioconjugate Chem.* **2007**, *18*, 1176–1184.
27. Weber, P.; Ohlendorf, D.; Wendoloski, J.; Salemme, F. Structural Origins of High-Affinity Biotin Binding to Streptavidin. *Science* **1989**, *243*, 85–88.
28. Choi, Y. S.; Yoon, C. W.; Lee, H. D.; Park, M.; Park, W. Efficient Protein–Ligand Interaction by Guaranteeing Mesospacing between Immobilized Biotins. *Chem. Commun.* **2004**, 1316–1317.
29. Tokuhisa, H.; Liu, J. a.; Omori, K.; Kanesato, M.; Hiratani, K.; Baker, L. A. Efficient Biosensor Interfaces Based on Space-Controlled Self-Assembled Monolayers. *Langmuir* **2009**, *25*, 1633–1637.
30. Lehmann, E. L.; D'Abrera, H. J. M. *Nonparametrics: Statistical Methods Based on Ranks*; Prentice-Hall, 1998.

31. Peterson, A. W.; Wolf, L. K.; Georgiadis, R. M. Hybridization of Mismatched or Partially Matched DNA at Surfaces. *J. Am. Chem. Soc.* **2002**, *124*, 14601–14607.
32. Sakata, T.; Maruyama, S.; Ueda, A.; Otsuka, H.; Miyahara, Y. Stable Immobilization of an Oligonucleotide Probe on a Gold Substrate Using Tripodal Thiol Derivatives. *Langmuir* **2007**, *23*, 2269–2272.
33. Whitesell, J. K.; Chang, H. K. Directionally Aligned Helical Peptides on Surfaces. *Science* **1993**, *261*, 73–76.
34. Hegner, M.; Wagner, P.; Semenza, G. Immobilizing DNA on Gold via Thiol Modification for Atomic Force Microscopy Imaging in Buffer Solutions. *FEBS Lett.* **1993**, *336*, 452–456.
35. Hutter, J. L.; Bechhoefer, J. Calibration of Atomic-Force Microscope Tips. *Rev. Sci. Instrum.* **1993**, *64*, 1868–1873.
36. Preiner, J.; Ebner, A.; Chtcheglova, L.; Zhu, R.; Hinterdorfer, P. Simultaneous Topography and Recognition Imaging: Physical Aspects and Optimal Imaging Conditions. *Nanotechnology* **2009**, 20.